JACS
JOURNAL OF THE AMERICAN CHEMICAL SOCIETY
Communication
pubs.acs.org/JACS

Tuning the Luminescence of Metal–Organic Frameworks for Detection of Energetic Heterocyclic Compounds

Yuexin Guo,[†] Xiao Feng,*[,†] Tianyu Han,[‡] Shan Wang,[†] Zhengguo Lin,[†] Yuping Dong,[‡] and Bo Wang*[,†]

[†]Key Laboratory of Cluster Science, Ministry of Education of China, School of Chemistry, Beijing Institute of Technology, 5 South Zhongguancun Street, Beijing 100081, P. R. China

[‡]College of Materials Science & Engineering, Beijing Institute of Technology, 5 South Zhongguancun Street, Beijing 100081, P. R. China

Supporting Information

ABSTRACT: Herein we report three metal–organic frameworks (MOFs), TABD-MOF-1, -2, and -3, constructed from Mg^{2+}, Ni^{2+}, and Co^{2+}, respectively, and deprotonated 4,4′-((*Z*,*Z*)-1,4-diphenylbuta-1,3-diene-1,4-diyl)dibenzoic acid (TABD-COOH). The fluorescence of these three MOFs is tuned from highly emissive to completely nonemissive via ligand-to-metal charge transfer by rational alteration of the metal ion. Through competitive coordination substitution, the organic linkers in the TABD-MOFs are released and subsequently reassemble to form emissive aggregates due to aggregation-induced emission. This enables highly sensitive and selective detection of explosives such as five-membered-ring energetic heterocyclic compounds in a few seconds with low detection limits through emission shift and/or turn-on. Remarkably, the cobalt-based MOF can selectively sense the powerful explosive 5-nitro-2,4-dihydro-3*H*-1,2,4-triazole-3-one with high sensitivity discernible by the naked eye (detection limit = 6.5 ng on a 1 cm^2 testing strip) and parts per billion-scale sensitivity by spectroscopy via pronounced fluorescence emission.

Metal–organic frameworks (MOFs) are well-defined crystalline solids constructed from metal ions and organic linkers via covalent bonds.[1] Because of the tremendous choices of metal nodes and organic linkers, the optical properties of MOFs can be engineered. Such unique characteristics, as well as structural predictability and well-defined environments for luminophores either on the skeletons or inside the pores, allow for the use of luminescent MOFs as optical materials in various fields, especially chemo/biosensing applications.[2] A number of luminescent MOFs have been utilized to detect volatile organic compounds, small molecules, and energetic materials.[2,3] However, most sensors explored to date are based on energy transfer between host and guest molecules, which results in optical signal "turn-off" by fluorescence quenching. Such turn-off MOF sensors show intrinsic limitations, such as a lack of sufficient chemical selectivity and sensitivity. A long-sought goal for MOF sensors is to obtain a shift of an existing emission peak or, even better, the evolution of a new emission peak from a dark background (fluorescence "turn-on") because of its significant advantages, i.e., improved detection limit and selectivity, enhanced visible distinguishability, and so on.[2b,e,4]

Fluorophores with aggregation-induced emission (AIE) characteristics, which show no emission or weak emission in dilute solutions but are brightly fluorescent upon aggregation, offer great opportunities for the design of fluorescence turn-on probes.[5] Recently, several AIE MOFs constructed via self-assembly of tetraphenylethene derivatives and metal cations (Zn^{2+}, Mg^{2+}, or Zr^{4+}) have been reported to possess high fluorescent quantum yields (Φ_F) due to the restriction of intramolecular motion.[6] Although these AIE MOFs exhibit sensing abilities toward ammonia or volatile organic compounds, actual turn-on detection is still not achieved from the inherent pronounced fluorescence of the framework.

Herein we present a novel strategy to design MOF probes for turn-on detection applications by employing organic struts with the AIE feature and metal nodes with distinct outer-shell electron configurations. Coordination of 4,4′-((*Z*,*Z*)-1,4-diphenylbuta-1,3-diene-1,4-diyl)dibenzoic acid (TABD-COOH), an AIE fluorophore developed by us,[7] with Mg^{2+} produces the strongly luminescent MOF TABD-MOF-1 (Φ_F = 38.5%). Moreover, altering the metal ion from Mg^{2+} to Ni^{2+} and Co^{2+} with incomplete d subshells yields the barely fluorescent and completely nonfluorescent MOFs TABD-MOF-2 and TABD-MOF-3, respectively. Such dimmed fluorescence can be attributed to the stronger ligand-to-metal charge transfer (LMCT) effect and allows turn-on detection of guest molecules. These three TABD-MOFs with different inherent emissions were further used for selective sensing of five-membered-ring energetic heterocyclic compounds (5MR-EHCs), the detection of which is ever urgent but has not been realized by a fluorescent approach.

TABD-COOH with the (*Z*,*Z*) configuration was synthesized and isolated in three steps according to our previously reported procedure[7] in an overall yield of 51%. The AIE feature of TABD-COOH was evidenced by a significant increase in quantum yield in going from its THF solution (Φ_F = 1.28%) to the solid state (Φ_F = 69.60%).

The syntheses of the three TABD-MOFs were carried out by heating a solution mixture of TABD-COOH and $Mg(NO_3)_2 \cdot 6H_2O$, $Ni(NO_3)_2 \cdot 6H_2O$, or $Co(NO_3)_2 \cdot 6H_2O$ in *N*,*N*-dimethylformamide (DMF) at 85 °C for 1 day. The crystal structures

Received: September 7, 2014
Published: October 17, 2014

   dx.doi.org/10.1021/ja508962m | *J. Am. Chem. Soc.* 2014, 136, 15485–15488

were determined by single-crystal X-ray diffraction (SXRD). TABD-MOF-1 is composed of magnesium binuclear secondary building units (SBUs) (Figure 1a, left). Each SBU is connected

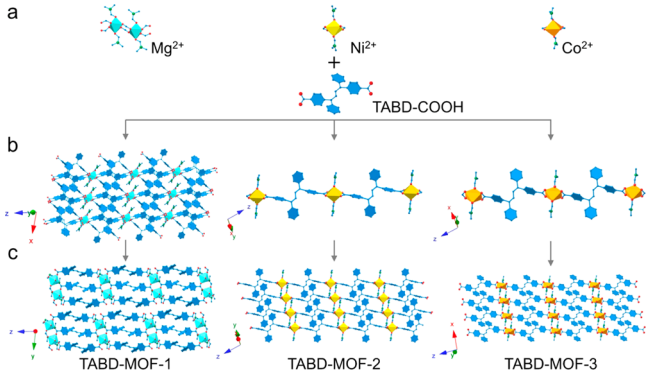

Figure 1. (a) Second building units (SBUs), (b) 2D sheets or 1D chains, and (c) crystal structures of TABD-MOFs. C, dark blue; O, red; N, green; Mg, sky blue; Ni, yellow; Co, orange. H atoms have been omitted for clarity.

to six deprotonated TABD-COOH linkers, and other coordination positions in the binuclear six-coordinate Mg(II) clusters are occupied by two O atoms from two DMF molecules. Overall, each SBU is linked to two neighboring SBUs by six deprotonated TABD-COOH ligands to form 2D sheets in the *xy* plane (Figure 1b, left). Furthermore, the 2D sheets in TABD-MOF-1 are propagated to form an extended 3D structure with the aid of C−H···π interactions rather than close π−π stacking (Figures 1c and 2a). Such close hydrogen-

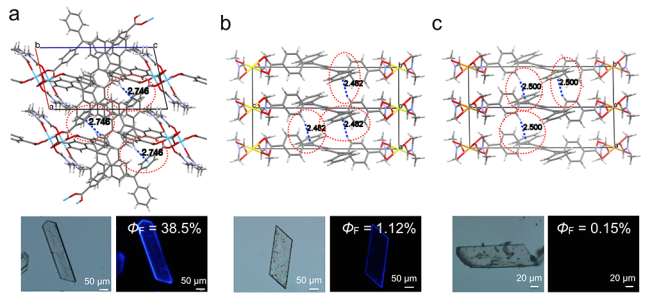

Figure 2. Views of C−H···π interactions in the crystal structures, bright-field images, and fluorescence images of (a) TABD-MOF-1, (b) TABD-MOF-2, and (c) TABD-MOF-3. C, gray; O, red; Mg, sky blue; Ni, yellow; Co, orange.

bonding interactions can efficiently restrict the rotations of the phenyl rings in the three MOFs, avoid close π−π interactions, lower the nonemissive energy lost, and thus block the nonradiative pathway.[5b,c,6a]

TABD-MOF-2 and TABD-MOF-3 are 1D MOFs in which deprotonated TABD-COOH ligands adopt a bis(bidentate) mode to link mononuclear metal ions. Each nickel ion or cobalt ion is coordinated to four carboxylate oxygen atoms from two deprotonated TABD-COOH molecules and two DMF molecules (Figure 1b, middle and right). As in TABD-MOF-1, C−H···π interactions conjugate the 1D chains to form extended 3D structures in TABD-MOF-2 and -3 (Figures 1c and 2b,c). The distances of the C−H···π interactions are 2.48 and 2.50 Å for TABD-MOF-2, and TABD-MOF-3, respectively. Powder X-ray diffraction (PXRD) patterns match well with those simulated from their SXRD data, confirming the purity of the TABD-MOFs (Figure S1 in the Supporting Information).

As shown in Figure 2, the diamond-shaped single crystals of the three TABD-MOFs exhibit distinct fluorescent behaviors. Strong luminescence of TABD-MOF-1 is observed at 441 nm, which is consistent with the crystalline solid-state ligand molecules (TABD-COOH). The Φ_F of TABD-MOF-1 is as high as 38.5%, a remarkable 30-fold enhancement of the fluorescent quantum yield compared with TABD-COOH molecules in THF solution. As expected, after the Mg^{2+} ions are replaced by paramagnetic metal ions (Ni^{2+} and Co^{2+}) to construct the other two MOFs, Φ_F is efficiently decreased (1.12% for TABD-MOF-2 and 0.15% for TABD-MOF-3). Especially for TABD-MOF-3, no emission is visible under illumination using a hand-held UV lamp at 365 nm (Figure 2c). Obvious hypsochromic shifts are observed in their emission spectra (Figure S2), demonstrating that LMCT transitions govern the inherent optical properties of the two MOFs and thus quench their fluorescence.

5MR-EHCs with high nitrogen content offer remarkable advantages over conventional energetic compounds, such as high heat of formation and rather low sensitivity toward friction and impact.[8] However, unlike the detection of some well-known carbon-based explosives [i.e., 2,4,5-trinitrotoluene (TNT), 1,3,5-trinitroperhydro-1,3,5-triazine (RDX), and cyclotetramethylene tetranitramine (HMX)], which can be readily realized through the fluorescent approach,[2b,4,9] the demand for a facile and sensitive detection method for 5MR-EHCs is ever urgent yet largely unmet. Various 5MR-EHCs (i.e., triazoles, tetrazoles, azoxyfurazans, and their derivatives, salts, and hybrid compounds)[8] possess distinct molecular structures, substituent groups, and orbital energies, and hence, the well-established fluorometric methods that are based on energy transfer or specific reaction show intrinsic limitations for the detection of these high-energy-density materials.

One feature these heterocyclic compounds have in common is the C═N and/or N═N bonds in the heterocyclic rings, which allows the dissociation of coordination bonds between carboxylate groups and metal ions in MOFs through competitive coordination substitution. Therefore, once a MOF skeleton constructed using AIE linkers with carboxylate groups is applied for detection of 5MR-EHCs, the AIE molecules will be released and subsequently reassemble to form emissive aggregates.

As a proof-of-concept experiment, we initially chose 5-nitro-2,4-dihydro-3*H*-1,2,4-triazole-3-one (NTO) as the target heterocyclic high-energy-density material (Figure S3a).[10] To evaluate the performance of these three TABD-MOFs for detection of NTO explosive, the MOF samples (~0.1 mg) were deposited on the surface of testing papers (Figure S3b). Then, spot tests using the above paper strips were carried out. THF solutions of NTO (10^{-3} mol/L, 10 μL) were placed on the paper strips to give a spot area of approximately 0.2 cm^2. As shown in Figure S4, dramatic emission changes for all three TABD-MOFs were observed within several seconds. The fluorescent color of TABD-MOF-1 changed from blue (λ_{max} = 441 nm) to green (λ_{max} = 456 nm), while that of TABD-MOF-2 altered from dim blue (λ_{max} = 435 nm) to bright green (λ_{max} = 456 nm). Particularly, a clear turn-on emission was triggered upon addition of NTO to TABD-MOF-3 (Figures S4 and S5). In blank tests, no obvious emission changes (wavelength or

dx.doi.org/10.1021/ja508962m | J. Am. Chem. Soc. 2014, 136, 15485−15488

intensity) were found upon exposure to THF. Furthermore, linkers alone could not sense NTO (Figures S9 and S10).

The visual fluorescence response of TABD-MOF-3 (<0.1 mg) to NTO at different concentrations in spot testing is shown in Figure 3a. The minimum amount of NTO detectable

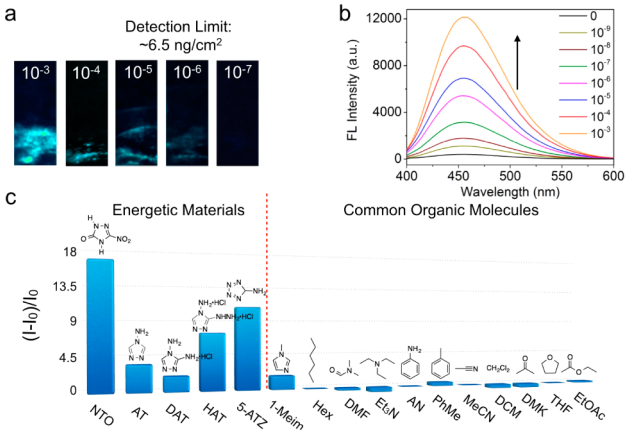

Figure 3. (a) Photographs of TABD-MOF-3-deposited paper strips upon addition of THF solution of NTO at different concentrations under UV light. (b) Fluorescence spectra of TABD-MOF-3 in THF upon addition of NTO solution at different concentrations followed by addition of hexane. (c) Fluorescence enhancement efficiencies ($(I - I_0)/I_0$) obtained from different analytes by TABD-MOF-3. Excitation wavelength: 360 nm.

by the naked eye is as low as 10 μL of a 1×10^{-6} M solution, corresponding to a visible detection limit of ca. 6.5 ng/cm^2. As shown in the fluorescence spectra of the test strips (Figure S6), the emission is enhanced drastically upon addition of NTO explosive. Interestingly, the addition of NTO solutions to TABD-MOF suspensions in THF resulted in no changes in the emission. Nevertheless, the emission was boosted when a large amount of hexane was added to the mixture (Figure S7). Fluorescence turn-on by NTO in THF/hexane could be quantitatively detected in the concentration range from 4×10^{-8} to 10^{-3} mol/L (Figures 3b and S7b) with a limit of detection as low as 4×10^{-8} mol/L. Although other spectrophotometric and chromatographic methods have been reported for the determination of NTO with high reusability and reproducibility,[11] the fluorescent method allows the rapid detection NTO by the naked eye.

To confirm the mechanism of NTO detection by TABD-MOFs, mass spectrometry (MS) and ^{1}H NMR and UV−vis spectroscopy were performed. In the MOF solutions with additional NTO explosive, the peaks attributed to the dissociated TABD-COOH molecules and NTO coordination compounds could be identified in both the MS spectra (Figure S8a,b) and ^{1}H NMR spectra (Figure S8c). Moreover, the UV−vis spectra (Figure S9b) and fluorescence spectra (Figure S9a) are in agreement with those of free TABD-COOH molecules in THF solution. This demonstrates that the TABD-MOFs barely retains its structural integrity upon addition of NTO because of the competitive coordination substitution, and thus free TABD-COOH molecules are released into the solutions. Upon evaporation of THF solvent during the paper strip tests or addition of hexane in the solution tests, the dissociated TABD-COOH molecules begin to aggregate, and the emission is boosted as a result of the restriction of intramolecular rotations[7] (Figure 4).

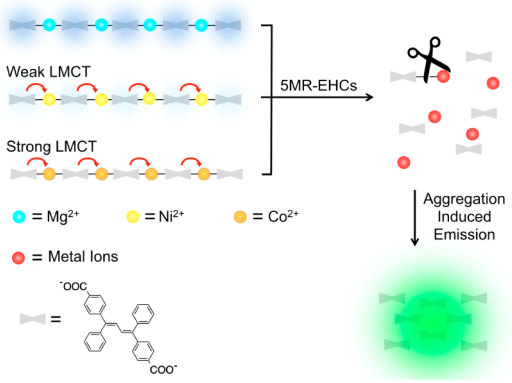

Figure 4. Schematic representation of the mechanism of the detection of energetic heterocyclic compounds by the three TABD-MOFs. LMCT: ligand-to-metal charge transfer.

To check the applicability and selectivity of TABD-MOF-3 for energetic heterocyclic compounds, both spot tests on paper strips (Figure S10) and fluorescence spectroscopy measurements in solution (Figures 3c and S11) were performed. No obvious emission changes were observed for common organic molecules and nitroaromatics, such as DMF, triethylamine (Et_3N), aniline (AN), toluene (PhMe), hexane (Hex), acetonitrile (MeCN), dichloromethane (DCM), acetone (DMK), THF, ethyl acetate (EtOAc), TNT, and HMX, indicating that $-NH_2$, C═O, $-NO_2$, and −OH groups, aromatic rings, aliphatic chains, and an alkalescent environment do not interfere with the sensing results. Consistent with our assumptions and previous results with NTO, 4*H*-1,2,4-triazol-4-amine (AT), 4*H*-1,2,4-triazole-3,4-diamine hydrochloride (DAT), 3-hydrazinyl-4*H*-1,2,4-triazol-4-amine dihydrochloride (HAT), and 5*H*-tetrazol-5-amine (5-ATZ), which are typical 5MR-EHCs and/or source materials for the synthesis of high-energy-density materials, can cause remarkable emission turn-on.

In conclusion, three newly designed TABD-MOFs with tunable fluorescent properties have been prepared. Through the use of metal nodes with different outer-shell electron configurations, both highly emissive and nonemissive MOFs were readily obtained. The original fluorescence of the organic linkers can be recovered through competitive coordination substitution. This simple strategy for the off/on response benefiting from both MOF design principles and AIE features is applicable to the efficient and selective detection of C═N- and/or N═N-containing heterocyclic explosives, which are high-energy-density materials or source materials for them. A disposable paper strip with a trace amount of TABD-MOFs on it can realize naked-eye-readable detection of highly dangerous 5MR-EHCs within several seconds with unprecedented detection sensitivity. The present new AIE-MOF method shows advantages of universality, high sensitivity, and ease of visualization and may shed light on the development of new probes for turn-on chemo/biosensing applications. Vapor detection applications are presently being studied, and the results will be reported in due course.

■ ASSOCIATED CONTENT

Supporting Information

Synthetic materials and instruments, synthetic methods, single-crystal data (CIF), and spectroscopic data. This material is available free of charge via the Internet at http://pubs.acs.org.

dx.doi.org/10.1021/ja508962m | J. Am. Chem. Soc. 2014, 136, 15485−15488

AUTHOR INFORMATION

Corresponding Authors

bowang@bit.edu.cn
fengxiao86@bit.edu.cn

Notes

The authors declare no competing financial interest.

ACKNOWLEDGMENTS

This work was financially supported by the 973 Program (2013CB834704), "1000 Plan (Youth)", and the National Natural Science Foundation of China (Grants 21404010 and 21201018).

REFERENCES

(1) (a) Kitagawa, S.; Kitaura, R.; Noro, S. *Angew. Chem., Int. Ed.* **2004**, *43*, 2334−2375. (b) Horike, S.; Shimomura, S.; Kitagawa, S. *Nat. Chem.* **2009**, *1*, 695−704. (c) Furukawa, H.; Cordova, K. E.; O'Keeffe, M.; Yaghi, O. M. *Science* **2013**, *341*, No. 1230444. (d) Férey, G. *Chem. Soc. Rev.* **2008**, *37*, 191−214. (e) Long, J. R.; Yaghi, O. M. *Chem. Soc. Rev.* **2009**, *38*, 1213−1214. (f) Zhou, H. C.; Long, J. R.; Yaghi, O. M. *Chem. Rev.* **2012**, *112*, 673−674.

(2) (a) Allendorf, M. D.; Bauer, C. A.; Bhakta, R. K.; Houk, R. J. *Chem. Soc. Rev.* **2009**, *38*, 1330−1352. (b) Hu, Z.; Deibert, B. J.; Li, J. *Chem. Soc. Rev.* **2014**, *43*, 5815−5840. (c) Lu, W.; Wei, Z.; Gu, Z. Y.; Liu, T. F.; Park, J.; Park, J.; Tian, J.; Zhang, M.; Zhang, Q.; Gentle, T., III; Bosch, M.; Zhou, H. C. *Chem. Soc. Rev.* **2014**, *43*, 5561−5593. (d) Cui, Y.; Yue, Y.; Qian, G.; Chen, B. *Chem. Rev.* **2012**, *112*, 1126−1162. (e) Kreno, L. E.; Leong, K.; Farha, O. K.; Allendorf, M.; Van Duyne, R. P.; Hupp, J. T. *Chem. Rev.* **2012**, *112*, 1105−1125.

(3) (a) Dong, M.-J.; Zhao, M.; Ou, S.; Zou, C.; Wu, C.-D. *Angew. Chem.* **2014**, *126*, 1601−1605. (b) Lin, R.-B.; Li, F.; Liu, S.-Y.; Qi, X.-L.; Zhang, J.-P.; Chen, X.-M. *Angew. Chem.* **2013**, *125*, 13671−13675.

(4) Germain, M. E.; Knapp, M. J. *Chem. Soc. Rev.* **2009**, *38*, 2543−2555.

(5) (a) Luo, J. D.; Xie, Z. L.; Lam, J. W. Y.; Cheng, L.; Chen, H. Y.; Qiu, C. F.; Kwok, H. S.; Zhan, X. W.; Liu, Y. Q.; Zhu, D. B.; Tang, B. Z. *Chem. Commun.* **2001**, 1740−1741. (b) Hong, Y.; Lam, J. W. Y.; Tang, B. Z. *Chem. Soc. Rev.* **2011**, *40*, 5361−5388. (c) Mei, J.; Hong, Y.; Lam, J. W. Y.; Qin, A.; Tang, Y.; Tang, B. Z. *Adv. Mater.* **2014**, *26*, 5429−5479. (d) Ding, D.; Li, K.; Liu, B.; Tang, B. Z. *Acc. Chem. Res.* **2013**, *46*, 2441−2453.

(6) (a) Shustova, N. B.; McCarthy, B. D.; Dincă, M. *J. Am. Chem. Soc.* **2011**, *133*, 20126−20129. (b) Shustova, N. B.; Cozzolino, A. F.; Dincă, M. *J. Am. Chem. Soc.* **2012**, *134*, 19596−19599. (c) Shustova, N. B.; Cozzolino, A. F.; Reineke, S.; Baldo, M.; Dincă, M. *J. Am. Chem. Soc.* **2013**, *135*, 13326−13329. (d) Zhang, M.; Feng, G.; Song, Z.; Zhou, Y.-P.; Chao, H.-Y.; Yuan, D.; Tan, T. T. Y.; Guo, Z.; Hu, Z.; Tang, B. Z.; Liu, B.; Zhao, D. *J. Am. Chem. Soc.* **2014**, *136*, 7241−7244.

(7) (a) Han, T.; Zhang, Y.; Feng, X.; Lin, Z.; Tong, B.; Shi, J.; Zhi, J.; Dong, Y. *Chem. Commun.* **2013**, *49*, 7049−7051. (b) Zhang, Y.; Han, T.; Gu, S.; Zhou, T.; Zhao, C.; Guo, Y.; Feng, X.; Tong, B.; Shi, J.; Zhi, J.; Dong, Y. *Chem.—Eur. J.* **2014**, *20*, 8856−8861.

(8) (a) Singh, R. P.; Verma, R. D.; Meshri, D. T.; Shreeve, J. M. *Angew. Chem., Int. Ed.* **2006**, *45*, 3584−3601. (b) Steinhauser, G.; Klapötke, T. M. *Angew. Chem., Int. Ed.* **2008**, *47*, 3330−3347. (c) Joo, Y.-H.; Shreeve, J. M. *Angew. Chem., Int. Ed.* **2009**, *48*, 564−567. (d) Wang, R.; Xu, H.; Guo, Y.; Sa, R.; Shreeve, J. M. *J. Am. Chem. Soc.* **2010**, *132*, 11904−11905. (e) Zhang, J.; Shreeve, J. M. *J. Am. Chem. Soc.* **2014**, *136*, 4437−4445.

(9) (a) Thomas, S. W.; Joly, G. D.; Swager, T. M. *Chem. Rev.* **2007**, *107*, 1339−1386. (b) Nagarkar, S. S.; Joarder, B.; Chaudhari, A. K.; Mukherjee, S.; Ghosh, S. K. *Angew. Chem., Int. Ed.* **2013**, *52*, 2881−2885. (c) Andrew, T. L.; Swager, T. M. *J. Am. Chem. Soc.* **2007**, *129*, 7254−7255.

(10) (a) Brill, T. B.; Gongwer, P. E.; Williams, G. K. *J. Phys. Chem.* **1994**, *98*, 12242−12247. (b) Singh, G.; Felix, S. P. *J. Hazard. Mater.* **2002**, *90*, 1−17. (c) Sinditskii, V. P.; Smirnov, S. P.; Egorshev, V. Y. *Propellants, Explos., Pyrotech.* **2007**, *32*, 277−287.

(11) Can, Z.; Üzer, A.; Tekdemir, Y.; Erçağ, E.; Türker, L.; Apak, R. *Talanta* **2012**, *90*, 69−76.